TEMPORAL EVOLUTION OF ARTIFICIAL SOLAR GRANULES

S. R. O. PLONER and S. K. SOLANKI
Institute of Astronomie, ETH Zentrum, 8092 Zürich, Switzerland

A. S. GADUN
Main Astronomical Observatory of Ukrainian, Goloseevo, 252650 Kiev-22, Ukraine

A. HANSLMEIER
Institut für Astronomie, Universitätsplatz 5, A-8010 Graz, Austria

Abstract. We study the evolution of artificial granulation on the basis of 2-D hydrodynamical simulations. These clearly show that granules die in two different ways. One route to death is the well known bifurcation or fragmentation of a large granule into 2 smaller ones (exploding granules). The other pathway to death is characterized by merging intergranular lanes and the accompanying dissolution of the granule located between them. It is found that the lifetime and maximum brightness is independent of the way in which granules evolve and die. They clearly differ in size, however, with exploding granules being in general significantly larger.

Key words: Solar Convection, Solar Granulation, Radiation-Hydrodynamic Simulation

1. Introduction

Most solar elemental abundances refer to the solar photosphere. This lowest atmospheric layer is structured by overshooting convection visible as granulation (see Spruit *et al.*, 1990 for a review). The elemental abundances determined from photospheric spectral lines may be inaccurate, if the properties of the granules are not taken into account. We present here a theoretical investigation aimed at better understanding the evolution of granules and hence of the inhomogeneities responsible for introducing inaccuracies into abundance measurements.

Direct numerical integration of the radiation hydrodynamic equations has provided new insight into the physical processes involved in solar granular convection (e.g. Nordlund, 1985; Stein *et al.*, 1989; Rast, 1993; Freytag *et al.*, 1996). A 2-D fully compressible radiation hydrodynamic simulation of solar granulation (free upper and lower and cyclic lateral boundary conditions) and of the corresponding synthetic spectra underlies the present investigation. Details of the simulation have been given by Gadun *et al.* (1995, 1996, 1998). In order to be able to follow the evolution of a sufficiently large number of granules we decided to reduce the number of spatial dimensions to 2. The computational domain covers horizontally $\approx$18 Mm real solar distance (512 grid points with 35 km spacing) and vertically $\approx$2 Mm (58 grid points with the same spacing). The evolution of the gas in the computational domain has been simulated for 5 hours real solar time in 0.3 s steps.

Space Science Reviews **85**: 261–268, 1998.

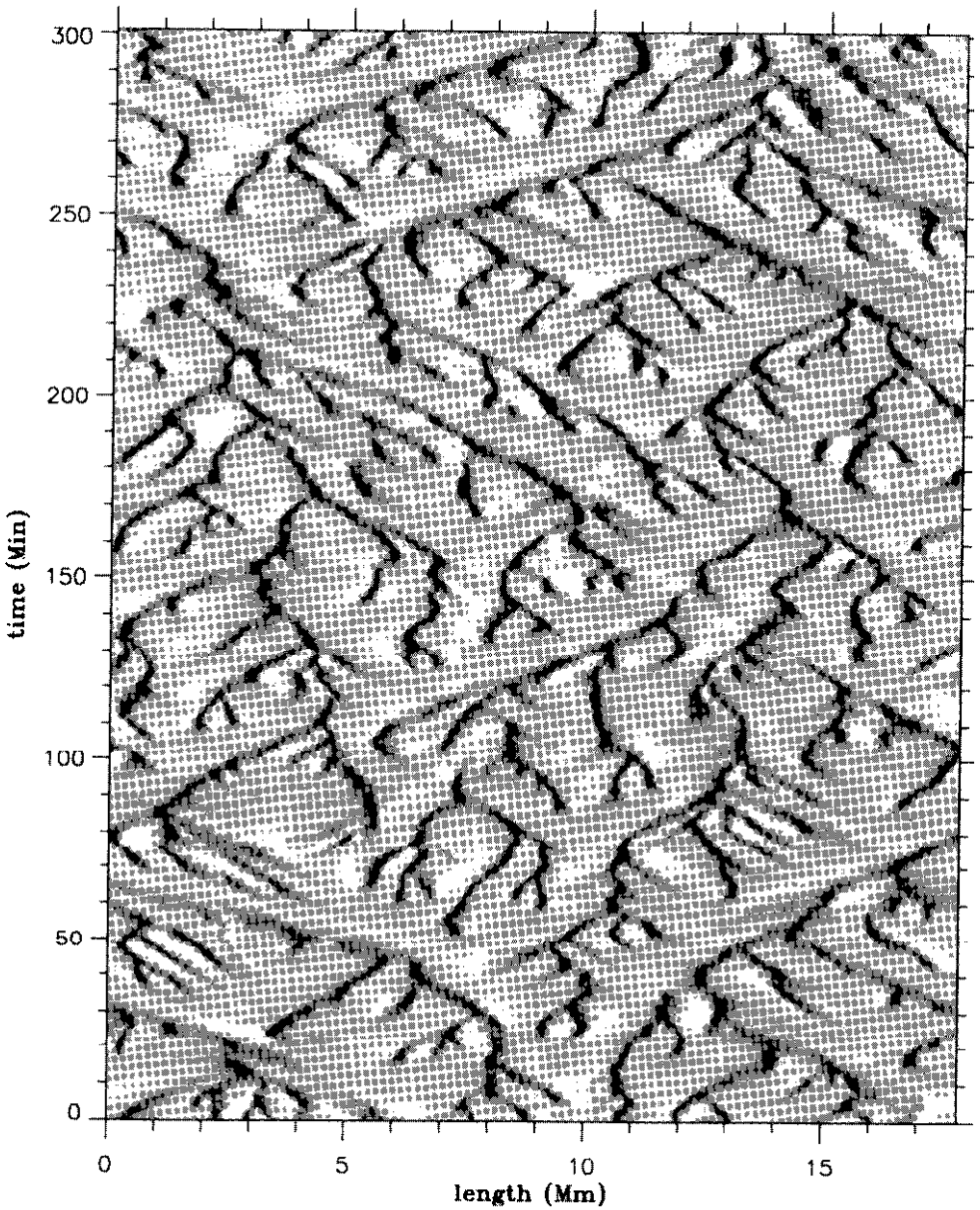

Figure 1. **Temporal evolution of the longitudinal velocity of artificial granulation.** Regions with dark shading indicate downflows, regions with light shading upflows. The intergranular lanes may start and merge but they never end. Merging intergranular lanes enclose a dying granule (which we call a *dissolving granule*). A starting intergranular lane marks both the death of a *fragmenting* or *exploding granule* and the birth of two new granules.

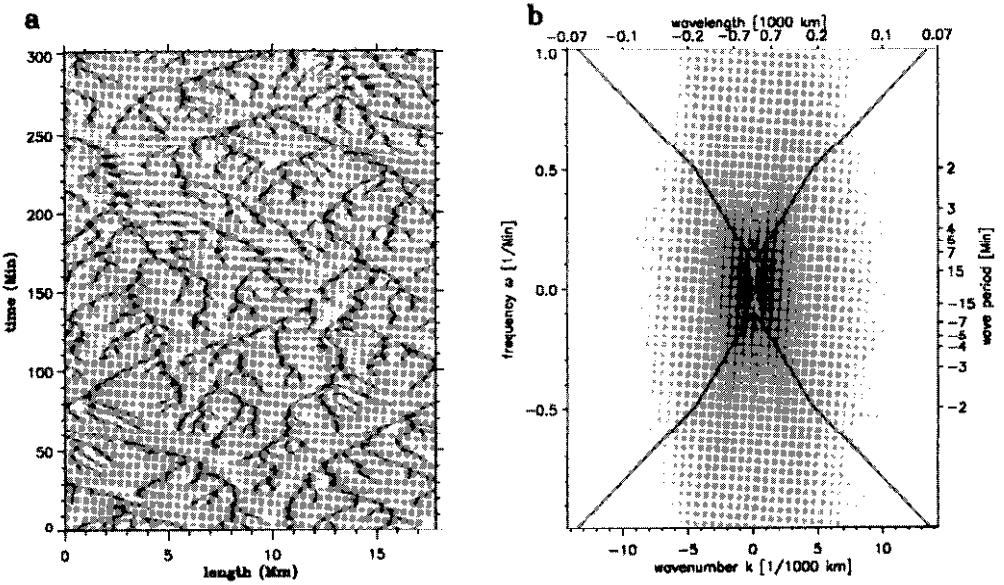

Figure 2. **Space–time filtering of the granular evolution**. Figure 2a displays the same as Fig. 1 but without space–time filtering. Figure b is the 2-D Fourier transformation of Fig. 2a. The neglect of the k-ω contribution in the inner part of the solid lines removes the p-modes. Figure 1 is the inverse Fourier transform of Fig. 2b, carried out after the filtering.

2. Analysis and Results

2.1. Removal of p-mode Oscillation

Figure 1 displays the temporal evolution of the granules seen in the longitudinal velocity component taken at a constant height just slightly below the average formation height of the visible continuum. The thin dark structures correspond to downflows and the bright regions to upflows. The emergent continuum intensity has also been calculated (not shown). The pattern formed by the continuum intensity shows no significant differences relative to the longitudinal velocity structure. Figure 1 has been "cleaned" from the influence of p-modes. As seen in Fig. 2a, p-modes are prominent in the simulation and may locally falsify the granular structure by, e.g., the introduction of an effective upflow in an intergranular lane. The vertical velocity and also the pressure are parameters which are strongly influenced by the p-modes. Note that the influence of the p-modes on the atmosphere relative to that of granulation increases rapidly with height. In order to be able to study granulation unaffected by oscillations we applied a 2-D Fourier transformation to Fig. 2a. The transformed image is shown in Fig. 2b. Upon close inspection power ridges due to the 5 and 3 minutes oscillations can be identified in the k-ω diagram. The p-modes are then filtered by setting the transformation to zero in the part of the k ω diagram lying in the inner part of the triangles (after apodization). Figure 1

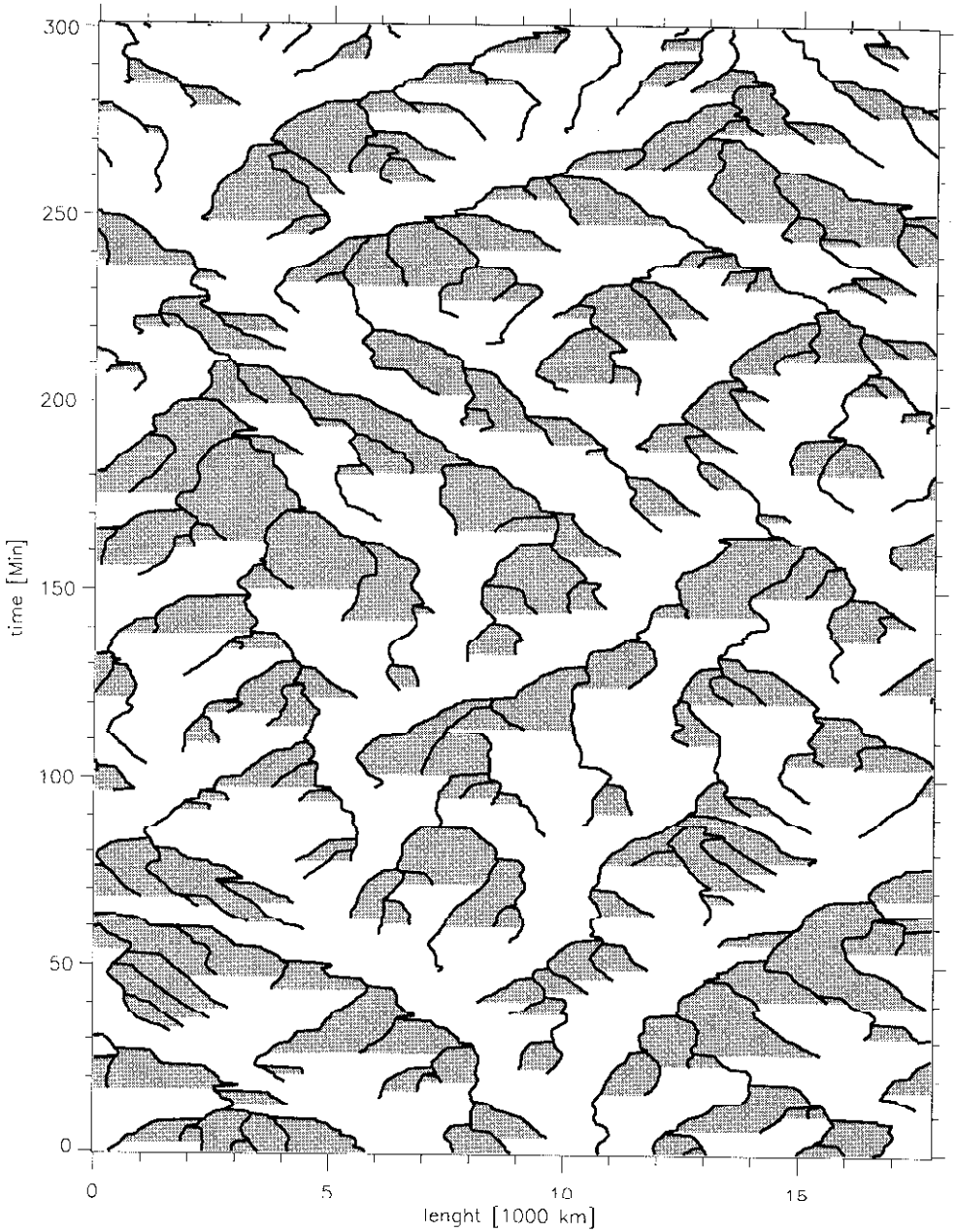

Figure 3. **Skeleton of the intergranular lanes** extracted from Figure 1 (solid curves). The shaded areas mark granules that end by dissolution while the remaining area is covered by fragmenting granules.

is then obtained by inverse Fourier transformation. This technique was pioneered for the analysis of high resolution observations (Title *et al.*, 1986). Note that not only is the granulation now more clearly visible, but higher frequency propagating waves, which had earlier been swamped by the p-modes are now uncovered.

2.2. Fragmenting and Dissolving Granules

In this presentation we focus on a statistical analysis of the temporal evolution of granulation. To this end we need to define the boundaries, as well as the birth and death of a granule. We have used the longitudinal velocity component taken at a fixed height to define these quantities. A granule is the upflowing structure between two adjacent downflow lanes (intergranular lanes). Hence for the purpose of the present analysis we can reduce the 3 dimensional data set (2 space and 1 time dimensions) to a more tractable 2 dimensional data set (1 horizontal and 1 time dimension).

Obviously, the granules and intergranular lanes exhibit a complementary temporal behaviour. Intergranular down-flowing lanes on the one hand often merge but never end although new lanes start. Granules, on the other hand, often end, but are only formed from the parts of fragmenting granules. Each time at the start of a new lane a granule splits into 2 (or more) smaller granules (fragmentation). This is a well studied route to granule death (e.g. Muller, 1989; Rast, 1993). Figure 1 also shows that most inter-granular lanes merge together. This corresponds to the death of the granule which is enclosed by the merging lanes. We call them dissolving granules (cf. Hirzberger *et al.*, 1997, for an observational study of small and large granules).

Figure 1 naturally leads to the characterization of granules by their mode of death. It is also obvious that the time evolution of the size of fragmenters and dissolvers is opposite: fragmenting granules rapidly expand whereas dissolving granules shrink.

2.3. Comparison between the 2 Granule Species

We consider now the relative significance and properties of dissolving and fragmenting granules. Figure 3 (solid curves) shows the skeleton of the intergranular lanes determined from Fig. 1. For each time step we searched for regions of downflows. The skeleton of the intergranular lane is then assigned to the location of maximal downflow. To keep the image from becoming cluttered only lanes that last more than 3 time-steps (= 1.5 Min) have been accepted. This sets a lower limit on the lifetime of dissolving granules that we consider, but we estimate that no such extremely short-lived dissolving granules were present in the simulation. In order to free the comparison between the two types of granules from bias fragmenting granules have also only been counted if their lifetime lies above 1.5 Min.

Table I

Granule Statistics. Granules are only considered if their lifetime is larger than 1.5 Min. The total number of fragmenters before this correction is displayed in brackets. The sum of the percentages of the area coverage is less than 100% due to the exclusion of short lived granules.

granule type	dissolving granules	fragmenting granules
total number	218	199 (218)
mean lifetime	8.6 Min	7.7 Min
mean size	865 km	2236 km
'area coverage'	35%	63%

Table I displays the basic statistics of the two granule types. The number and lifetime of fragmenting and dissolving granules are the same (before removing too short-lived fragmenting granules). Note that the number of granules is the same at the end and the beginning of the simulation. Remembering that fragmentation creates and dissolution removes 1 granule, it is obvious that on average there must be the same number of fragmenting and dissolving granules.

The mean lifetime is lower for fragmenting granules. This is mostly caused by rapid successive fragmentations, which give rise to very short lived granules (between 2 such splittings). Both the area coverage and the average size of the granules states that the dissolvers are significantly smaller than the fragmenters.

We then determined the average size, lifetime and maximum brightness of each granule. The comparison of granular lifetimes with mean sizes (Fig. 4a) confirms that dissolving granules ("•" in Fig. 4a) are smaller than fragmenting granules ("○" in Fig. 4a), with very little overlap in size between the two families of granules. The exploders exhibit a much larger range of sizes than dissolving granules. Dissolving granules show a clear relationship between size and lifetime, while for exploders such a relation is less clear. The larger the dissolving granule the longer it lives on the average (Fig. 4b). In contrast, the lifetime of the largest fragmenting granules is short. The two granule species basically agree in maximum brightness and lifetime. Figure 4b suggests that the brightness range of dissolving granules is slightly larger, certainly in the low intensity regime. The main effects visible from Fig. 4b is that the maximum brightness of granules increases on average with their lifetime and that the scatter of the maximum brightness values decreases towards larger lifetimes. Both Fig.s 4a and b also show that the two species cover the same lifetime range. The correlation of the average and maximum size of the granules seen in Fig. 4c gives an impression of the change of size during its evolution. A significant fraction of the granules lies below but near the slanted line. Granules lie exactly on the line when their size remains unchanged throughout their evolution. This indicates that over most of their lifetime their size changes only slightly.

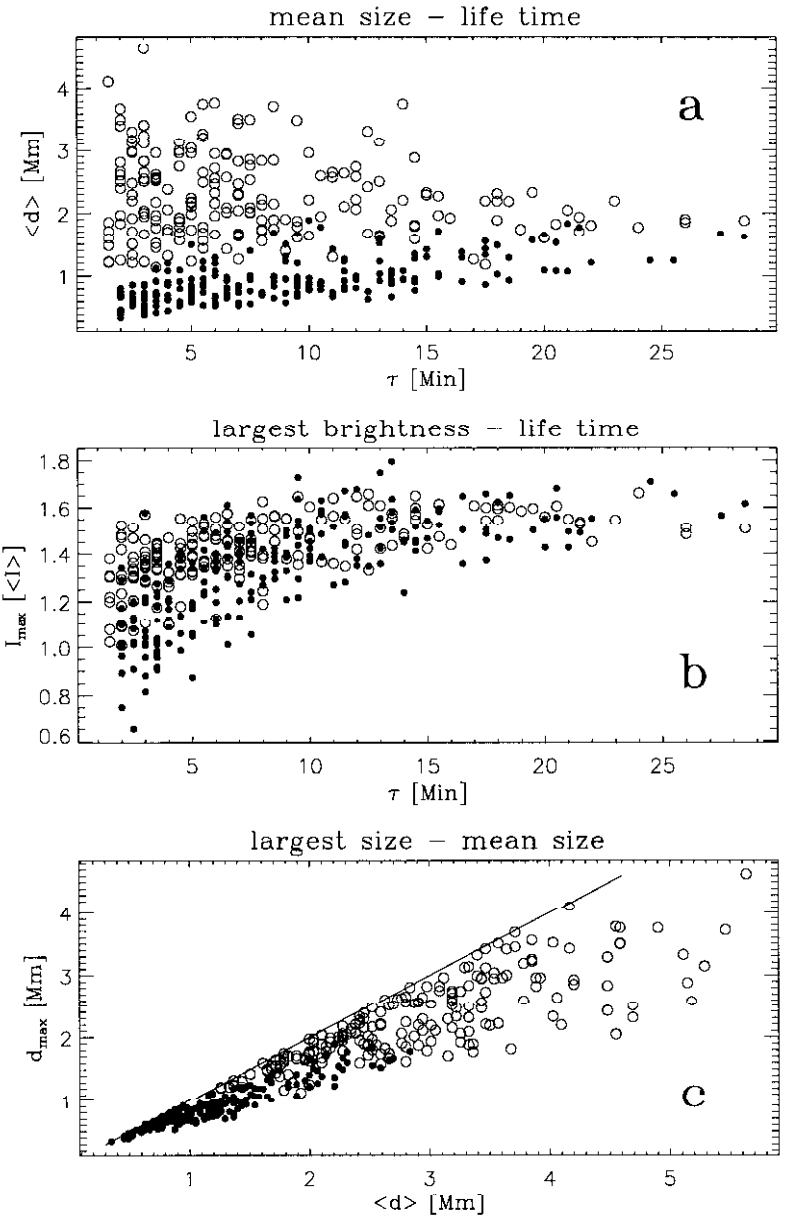

Figure 4. **Scatter plots** between the granule's average size $\langle d \rangle$ and lifetime τ (**a**), maximum brightness I_{max} and τ (**b**) and maximum size reached by the granule over its lifetime d_{max} versus $\langle d \rangle$ (**c**). Dissolving granules are marked by '•' (filled circle) and fragmenting granules by '○' (open circle).

3. Summary

We have investigated the temporal evolution of artificial granulation. p-modes are prominent in the simulation and were filtered out in order to study granulation

unaffected by oscillations. In addition to the well studied death of a granule by splitting (fragmenting or exploding granules) we have also studied granules that end by dissolution. This type of granule death is seen in Fig. 1 when two intergranular lanes merge. A comparison of the sizes, lifetimes and brightnesses shows that the dissolving granules differ mainly in size from the fragmenting granules, both types of granules having roughly the same lifetimes and maximum brightness.

Note that our study is limited to 2 spatial dimensions and that the properties of granulation in 3-D is different. Nevertheless, granules are known to split into different parts and some counteracting process must be at work in order to keep the number of granules finite. We therefore intend to continue studying the 2-D evolution of granules, in particular that of merging granules, with the aim of obtaining a better physical understanding of the underlying mechanisms.

References

Freytag, B., Ludwig, H.-G. and Steffen, M.: 1996, 'Hydrodynamical models of stellar convection. The role of overshoot in DA white dwarfs, A-type stars, and the Sun', *Astron. Astrophys.* **313**, 497.

Gadun, A.S. and Vorobyov, Yu.Yu.: 1995, 'Artificial Granules in 2-D Solar Models', *Sol. Phys.* **159**, 45.

Gadun, A.S. and Pikalov, K.N.: 1996, 'Two-Dimensional Hydrodynamical Modeling of Solar Granules: The Power Spectrum of Simulated Granules', *Astron. Rep.* **40**, 578.

Gadun, A.S., Solanki, S.K., Ploner, S.R.O., Hanslmeier, A., Pikalov, K.N., and Puschman, K.: 1998, 'Scale Dependent Properties of Artificial Solar Granulation Derived from 2–D Simulations', *Astron. Astrophys.*, in preparation.

Hirzberger, J., Vázquez, M., Bonet, J.A., Hanslmeier, A. and Sobotka, M.: 1997, 'Time Series of Solar Granulation Images. I. Differences between Small and Large Granules in Quiet Regions', *Astrophys. J.* **480**, 406.

Muller, R.: 1989, 'Solar Granulation: Overview', in *Solar and Stellar Granulation*, eds. Rutten, R.J. and Severino, G., Kluwer Academic Press, C **263**, 101.

Nordlund, Å.: 1985, 'Solar Convection', *Sol. Phys.* **100**, 209.

Rast, M.P.: 1993, 'On the nature of "exploding" granules and granule fragmentation', *Astrophys. J.* **443**, 863.

Spruit, H.C., Nordlund, Å. and Title, A.M.: 1990, 'Solar Convection', *Annu. Rev. Astron. Astrophys.* **28**, 263.

Stein, R.F., Nordlund, Å. and Kuhn, J.R.: 1989, 'Convection and Waves', in *Solar and Stellar Granulation*, eds. Rutten, R.J. & Severino, G., Kluwer Academic Press, C **263**, 381.

Title, A.M., Tarbell, T.D., Simon,G.W. and the SOUP Team: 1986, 'White-light movies of the solar photosphere from the soup instrument on space lab 2', *Adv. Space Res.* **6**, 253.

Address for correspondence: S. R. O. Ploner, Institute of Astronomie, ETH Zentrum, 8092 Zürich, Switzerland